

# Chapter 5

## Improving the cooling efficiency of industrial electronic components with the use of planar porous heat sinks

*Adam Steckiewicz, Gabriela Druć and Jacek Maciej Stankiewicz  
Bialystok University of Technology, Faculty of Electrical Engineering*

The article presents an analysis of the cooling efficiency of planar porous heat sinks, dedicated to improve thermal operating conditions of some electronic components. A single axial coil, placed on the laminate and convectionally cooled by a 2D laminated heat sink, was examined. The coil was supplied by a low frequency electric current. The three-dimensional numerical model of an electronic system was computed using the finite element method (FEM). Three cases are considered, where the element was operating without additional passive cooling, with the heat sink formed as a homogeneous copper plate as well as the element combined with the planar heat sink with modified internal structure.

**Index terms:** temperature distribution, printed circuit board, passive cooling, thermal energy efficiency

### Introduction

Power and industrial electronics grapple with the efficient cooling of electronic components and elements which are often enclosed in the smallest possible packages [1, 2]. The reduction of energy consumption by electric devices as well as constant demand for their effective work, force designers to utilize passive, instead of active, cooling structures [3] in the most sensitive parts of a circuit. The most popular plate and fin heat sinks, including those with complex project and implementation based on the 3D printing technique [4], are relatively massive and occupy a lot of space. Additionally, in the case of electronic elements with round shapes, one may find some difficulties with assembling a cooling and operating device together. This indicates that solutions which allow cooling electronic components with minimal cost, sizes and energy consumption are needed [5].

The most popular methods of dissipating the heat are additional passive structures. There are many solutions, such as thermal vias system filled with a high thermal conductivity material [6, 7] or planar, thermally conductive plates for increasing effective surface which dissipate heat from the electronic elements [8]. They are placed directly on or under the cooled element [9, 10] as well as on the other side of the printed circuit board (PCB) and connected with an element by thermal bridges. Those solutions dissipate lower power (less than several watts [11]) than fin heat sinks or active cooling; however their compact and build-in laminate structure allows for an application in systems with complex geometry.

The determination of an element's temperature during the steady state, under given ambient conditions, gives an ability to estimate its reliability and stability. There are several methods of temperature field analysis, such as analytical [12] and numerical approaches [13, 14], where calculations are carried out in the time-domain or steady state in systems characterized by heterogeneous thermal conductivity distribution. Utilizing an electrical-analog model, it is possible to analyze thermal effects using a lumped model [15]. Thermal resistance and capacity can be determined, for example on the basis of a comparison with measurement results or by identification technique using optimization methods [16]. Every overrun of critical temperature for a considered system may lead to thermal damage (e.g. local melting of the structure) or disturbances of the system and surrounding objects [9].

Reduced size (order of mm) and round geometry (small contact surface with a cooling device) may introduce difficulties with dissipation of generated or accumulated heat. One of the solutions is "printing" flat, thermally conductive structure under the cooled element [11]. Uniform lamina [2] or a "dog bone" plate [1] are exemplary solutions. If such a heat sink is placed on PCB, then etching the copper layer may lead to a structure consisting of periodically arranged pores inside the cooling plate, which will increase effective surface dissipating heat, thereby reducing the temperature of an electronic element [16].

In this paper we analyze an exemplary part of an electronic circuit with an axial coil. The heat is dissipated from the element by natural convection. We discuss the cases without passive cooling and configurations where planar porous heat sinks with modified internal design were applied. The aim of the study is to investigate the efficiency of this type of passive cooling structures. On the basis of the obtained results, the optimum structure is determined, where the terms of decreasing the coil's temperature and reducing material are the most crucial. The element's temperature and thermal field distribution depending on the ambient temperature, heat sink design and supply current are shown and characterized.

# Methods

## Electric and thermal field analysis

The operating conditions of components within the electrical system satisfy the overall power balance

$$Q_I + Q_G - Q_O - Q_A = 0. \tag{5.1}$$

Undesirable temperature change in an element is a result of its unbalance, where both input  $Q_I$  and generated power  $Q_G$  have to be equal to output power  $Q_O$ . The accumulated power  $Q_A$  is a difference between them. A decrease in the temperature value of the considered element is directly related with the decrease of  $Q_A$ . Additionally, the parasitic interactions inside the system are indirectly limited. Decreasing the temperature statistically increases mean time between failures as well as improves the efficiency of entire system. Then, prolonged work of the element is possible for provided power supply parameters or even at insignificant overload.

The analysis was focused on hybrid systems with surface-mount technology. The input power  $Q_p$ , resulting from thermal conduction between packaged components, consists of the heat conducted to an element and transmitted by other interactions (e.g. radiation). These factors are highly dependent on the system's geometry and casing. The impact of parasitic effects has been taken into account indirectly, by assuming the ambient temperature  $T_{ext}$ . The power dissipated in components surrounding the considered element will increase the internal temperature and cause a general deterioration of the heat transfer conditions.

Heat power generation is a result of the changes of energy, occurring due to an electric power supply and related with parasitic effects. Hence, the generated power  $Q_G$  characterizes possible changes in temperature distribution resulting from energy transformations. In the case of an axial coil the generated power consists of eddy current losses, hysteresis losses and the heat from the alternating current flowing through resistive material (winding). The power  $Q_G$  is also affected by phenomena related to thermal and electromagnetic field interactions.

The power generated in the system is dissipated as a result of the conduction, convection and radiation phenomena. The purpose of the presented technical solution is to increase power  $Q_O$ , dissipated from the element by introducing build-in planar heat sinks integrated with PCB. A heat sink is a part of laminate, where its geometry and layout (circuit paths placed at the bottom of a plate) are intended to increase conducted heat and transfer it to the ambient by convection and radiation.

The discussed phenomena are described by differential equations, which take into account material heterogeneity. The voltage distribution  $V$  in [V] satisfy the differential equation

$$\nabla \cdot (\sigma \nabla V) = 0, \quad (5.2)$$

where  $\sigma$  is electric conductivity in [S/m]. The vector of a current density distribution  $\mathbf{J}$  in [A/m<sup>2</sup>] inside the element is defined as

$$\mathbf{J} = \sigma \mathbf{E}, \quad (5.3)$$

where:

$\mathbf{E}$  – electric field vector in [V/m].

Taking into account only conduction currents, the power density distribution  $p$  in [W/m<sup>3</sup>] is described by a formula

$$p = \frac{|\mathbf{J}|^2}{\sigma}. \quad (5.4)$$

Due to low-frequency current, expected values of magnetic induction and application of a ferrite core, the eddy current and hysteresis losses were omitted. Their values, based on analytic calculations, did not exceed 1.16% of the ohmic losses. From the perspective of the analysis of thermal working conditions, taking these losses into account does not change the general assumptions and conclusions. An increase in considered power losses was observed in an area close to the ohmic loss. On this basis the temperature  $T$  in [°C], in thermal steady state, can be calculated using

$$\nabla \cdot (\lambda \nabla T) = -p, \quad (5.5)$$

where:  $\lambda$  is the thermal conductivity of a material in [W/mK].

We have considered conjugate phenomena occurring in electric and thermal fields. The temperature distribution in the system was described by (5.5) and solved on the basis of the calculated current density values using (5.2) and (5.3).

## Numerical model of the system

We have considered the part of electronic system (Fig. 5.1) with the element mounted on a laminate. Both working conditions as well as axial coil  $\Pi e$  of the length  $de = 15$  mm and base diameter  $\Phi e = 7.5$  mm were analyzed. The coil, covered by epoxy resin, had an internal ferrite core and winding with resistance of  $R = 1.4 \Omega$ .

The coil was mounted in the central part of the system, whose base  $\Pi p$  was an insulator (FR-4) with dimensions  $dx \times dy \times dz$  equal to  $25 \times 25 \times 1$  mm, respectively. The copper contacts  $\Pi s$  of a thickness  $dl = 0.07$  mm provided current supply to the element, connected to contacts  $\Pi s$  by leads  $\Pi d$  (diameter  $\Phi d = 0.7$  mm). Typical layout was complemented by a printed copper heat sink, introduced as an area  $\Pi r$  with dimensions of  $de \times dy \times dl$ . Its purpose was to dissipate the heat from  $\Pi e$  to the ambient with constant temperature  $T_{ext}$  by natural convection.

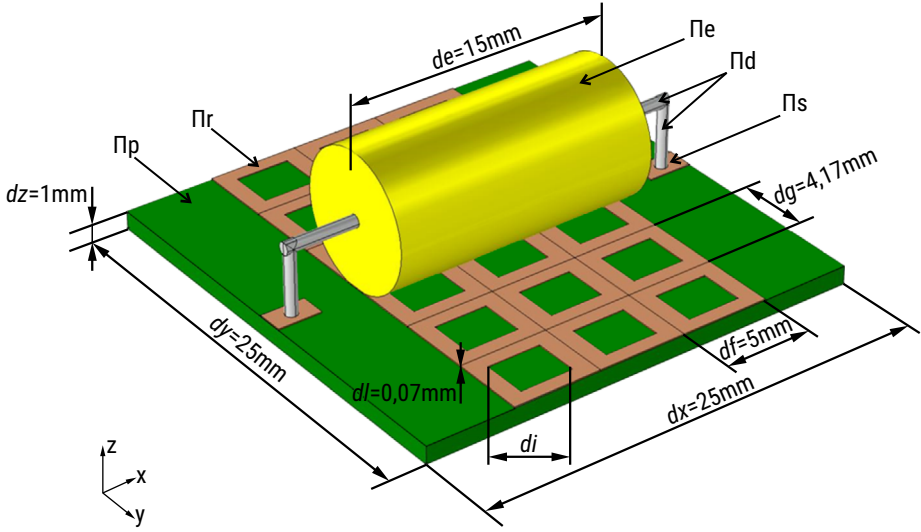


FIGURE 5.1. A view on the analyzed model with specified dimensions

The properties of the heat sink  $\Pi r$  with constant external dimensions were adjusted by modification of internal geometry. The structure was synthesized of 18 unit cells with dimensions  $df \times dg \times dl$  ( $5.00 \times 4.17 \times 0.07$  mm). The change of the diagonal of inner opening  $di$  modifies the geometry of the cell, which has a direct effect on reducing the amount of copper forming the heat sink and increasing the porosity of the cooling structure. Due to a specific geometry of the heat sink we are able to specify its structure using parameter

$$k_v = \frac{v_k}{v_c} = \frac{v_c - v_i}{v_c} = 1 - \frac{v_i}{df \cdot dg \cdot dl}, \quad (5.6)$$

where:

$v_k$  – volume of a single unit cell in  $[m^3]$ ;

$v_c$  – volume of uniform rectangular structure of a size  $df \times dg \times dl$  in  $[m^3]$ ;

$v_i$  – volume of an internal resection of a diagonal  $di$  in  $[m^3]$ .

This parameter characterizes the relation between the volume of the porous heat sink and the uniform cooling plate. For the homogeneous heat sink  $di = 0$  and  $k_v = 1$ , however, when the parameter is  $di = \sqrt{df^2 + dg^2}$ , the heat sink area is reduced to zero ( $k_v = 0$ ). By adjusting  $di$  value, it is possible to form a periodic array (Fig. 5.2), whose internal resection led to different cooling efficiency. In order to specify those properties of the heat sink we have proposed the parameter

$$e = \left[ 1 - \frac{T_{k,\max}}{T_{\vartheta,\max}} \right] \cdot 100\%. \quad (5.7)$$

The value of the temperature decrease effectiveness ( $e$ ) was calculated on the basis of:  $T_{k,max}$  – maximum temperature in the system cooled by optimal porous heat sink ( $k_v = 0.6$ ) in [°C] and  $T_{\vartheta,max}$  – maximum temperature in the system cooled by uniform heat sink ( $T_{\vartheta,max} = T_{j,max}$ ) or without any cooling structure ( $T_{\vartheta,max} = T_{b,max}$ ) in [°C].

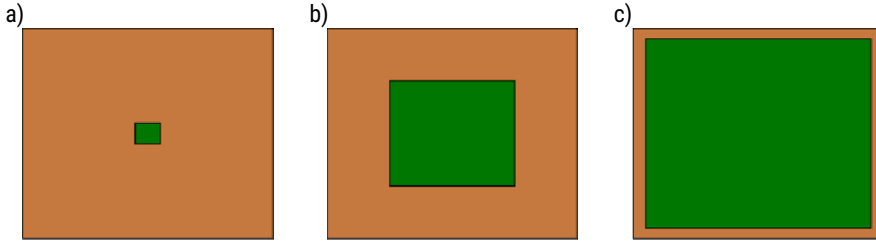


FIGURE 5.2. Exemplary periodic porous structures: a)  $di = 0.65$  mm ( $kv = 0.99$ ); b)  $di = 3.25$  mm ( $kv = 0.75$ ); c)  $di = 5.86$  mm ( $kv = 0.19$ )

The cooling conditions as well as the spectrum and effective value of supply current are known. The excitation is added to the numerical model as a constant current density  $\mathbf{J} = [J_x \ 0 \ 0]$  at terminals  $\Pi$ s of the element. Current density distribution as well as winding resistance determine the intensity and heat sources distribution in the system.

The Joule-Lenz heat dissipated in the electronic element is a distributed excitation for thermal field calculations, introduced upon the electric field distribution. In a steady state the thermal field depended on two key phenomena:

- heat conduction from generation area (coil interior) by contacts, material connections and thermal bridges to other objects in the system,
- heat transfer to the ambient by convection and radiation phenomena.

Therefore, according to the presented assumptions, the natural convection boundary conditions (no forced airflow) are assigned to the external boundaries of the system. The field problem is solved using the finite element method (FEM), where the presented model was discretized in a 3-dimensional space using a tetrahedral h-adaptive mesh.

## Results

### Impact of heat sink structure on element temperature

The considered system was computed numerically. The coil was supplied by low-frequency, nominal current. Temperature distribution at the surface of the model depends on the geometry of heat sink, localized on PCB and assembled with an electronic element (Fig. 5.3).

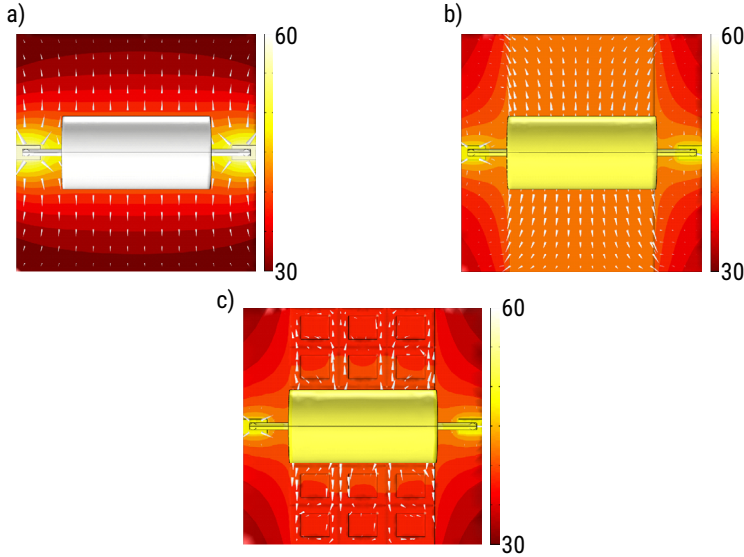


FIGURE 5.3. Temperature distribution ( $yz$  plane) and heat flow conducted through the surface of the structure at  $T_{ext} = 20^\circ\text{C}$  and  $I = I_n$  in the system: a) without passive cooling; b) cooled by uniform plate; c) cooled by porous heat sink

The system without the heat sink was characterized by the highest temperature values and heat flowing through copper contacts and leads (Fig. 5.3a). When the planar heat sink was placed, temperature distribution changed. For example, temperature values became more uniform at central area and the heat flux started to flow from the element to the upper and bottom edge through the heat sink's surface. However, the porous heat sink (Fig. 5.3c) had an approximately identical temperature as a laminate and heat flux appeared in the contact area between the element and the cooling plate. In the same region the most part of the heat was dissipated to the ambient.

For the assumed convective cooling conditions (natural, unforced convection) and current supply, the relation between the coil's maximum temperature and  $k_v$  (Fig. 5.4) were obtained. When  $k_v = 0$ , it meant that no heat sink was presented, however, for  $k_v = 1$  the heat sink was a homogeneous plate. Intermediate values of  $k_v$  characterized different porous heat sinks. In a steady state, the temperature of the element depended significantly on the cooling conditions (Fig. 5.4). The reference temperature  $T_0 = 65,954^\circ\text{C}$  was a maximum value at the surface of coil without any cooling structure at nominal operating conditions ( $I = I_n = 0.655\text{A}$  and  $T_{ext} = 20^\circ\text{C}$ ). When the amount of copper in the heat sink's structure increased, the temperature value decreased to  $0.8T_0$ . After  $k_v = 0.65$ , temperature raised to  $0.85T_0$ . When the coil was cooled by the uniform plate ( $k_v = 1$ ), the temperature was approximately 15% lower than without the heat sink. For some porous heat sinks ( $0.3 < k_v < 0.9$ ) we were able to achieve identical or more efficient cooling performance with a minimum temperature at  $k_v = 0.6$ . It was a result of dissipating heat by the entire heat sink and the laminate's surface as well as by internal side surfaces of the pores.

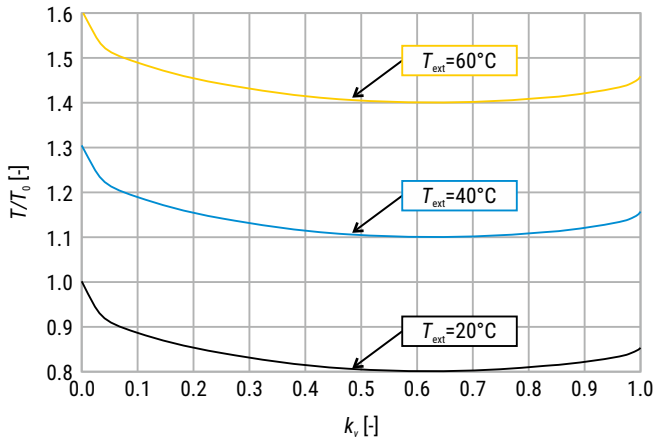


FIGURE 5.4. Maximum relative temperature for different heat sinks and  $T_{ext}$ ,  $l = ln$

Numerical computations were performed for three cooling conditions which were modeled as different ambient temperatures  $T_{ext}$ . A significant impact of  $T_{ext}$  on heat transfer in the system was clearly observed. In a steady state and at  $T_{ext} = 60^\circ\text{C}$ , the maximum temperature raised more than 60%, compared to the  $T_{ext} = 20^\circ\text{C}$  case. Additionally, a higher temperature decreased cooling effectiveness when any type of planar heat sink was used. For example, at  $k_v = 0.6$  and  $T_{ext} = 20^\circ\text{C}$  coil temperature was reduced by 20% compared to the case without the heat sink, although at  $T_{ext} = 40^\circ\text{C}$  the relative change was 15%.

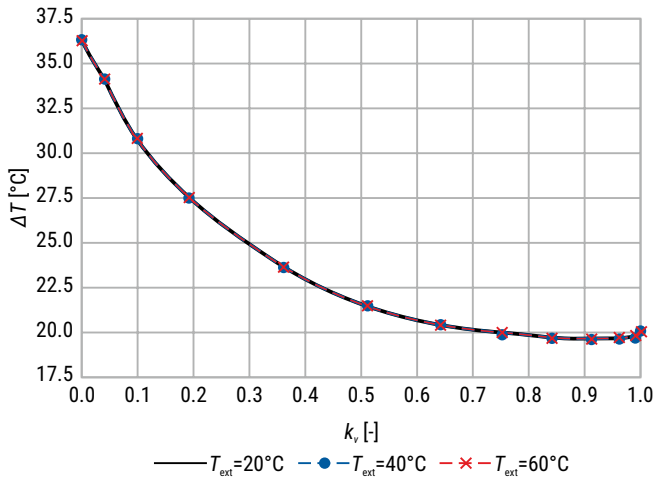


FIGURE 5.5. Temperature difference between the hottest and coolest point at the system surface for different heat sink structures at  $T_{ext} = \text{var}$  and  $l = ln$



We also defined the temperature difference  $\Delta T$  between the warmest (coil surface) and coolest (laminate surface) points of the system. The application of planar heat sinks has a positive impact on temperature difference reduction (Fig. 5.5). We observed an exponential decrease with increasing  $k_v$ . In an optimal case ( $k_v = 0.9$ ) maximum  $\Delta T = 19.5^\circ\text{C}$ , while at  $k_v = 0$ , the temperature difference was almost twice higher ( $\Delta T = 36^\circ\text{C}$ ). What is more, external temperature has no impact on  $\Delta T$  since curves for different  $T_{ext}$  overlapped each other. For  $k_v = 0.6$ , which was an optimal structure for cooling the element,  $\Delta T$  decreased to  $20.38^\circ\text{C}$ , which means that it was 2.44% less effective than the uniform heat sink.

### Current load impact on heat sink efficiency

From a practical point of view it is also important to define thermal operating conditions for electronic elements at different than nominal current supply. An ability to overload electronic elements is acceptable in particular situations; however it is the reason of possible damage to electronic components due to exceeding the recommended temperature range. For the considered coil, the maximum operating temperature was  $T_m = 125^\circ\text{C}$ . Numerical analysis for three variants:

- the system without the heat sink,
- the system with the uniform copper plate,
- the system with the optimal porous heat sink ( $k_v = 0.6$ ),

was intended to find the relation between mean temperature of the coil and supply current. The cooling effectiveness was also investigated for the coil supplied by current ranging from  $0 \div 2I_n$  (Fig. 5.6). We defined temperature decrease effectiveness when using the porous heat sink, with relation to the system without the cooling device and with the uniform heat sink (Fig. 5.7).

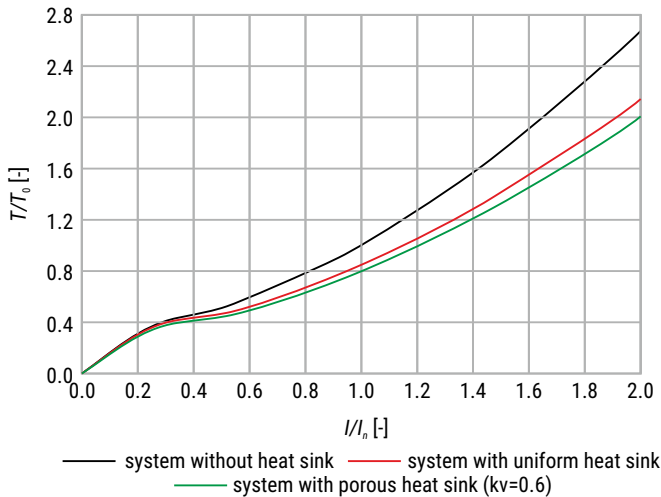


FIGURE 5.6. Maximum relative temperature for different supply currents and three types of the systems at  $T_{ext} = 20^\circ\text{C}$

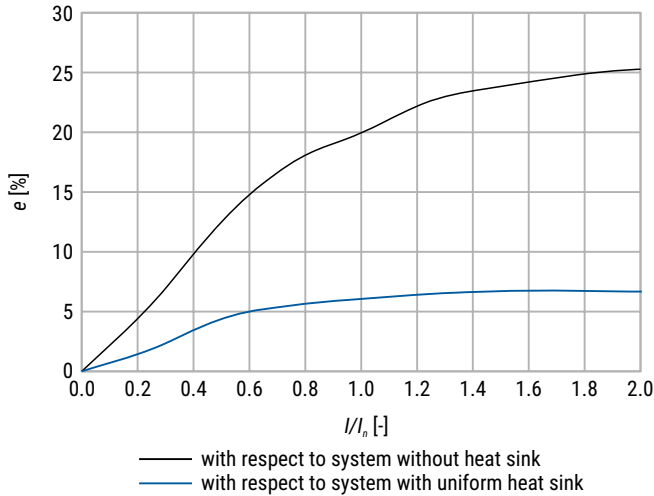


FIGURE 5.7. Temperature decrease effectiveness of a coil with porous heat sink for different supply currents at  $T_{ext} = 20^\circ\text{C}$

When the element was supplied by low-value current ( $0 \div 0.4I_n$ ), the coil's temperature was similar despite the heat sink structure (Fig. 5.6). For higher currents, differences in temperature values and a change in cooling effectiveness were observed. Maximum operating temperature for coil  $T_m = 1.9T_0$  was reached without the heat sink at  $I = 1.55I_n$ , however, with the porous heat sink it was  $I = 1.95I_n$ . In other words, the optimal planar heat sink gave an ability to overload the element by current almost twice higher than nominal, but still preserved the recommended temperature range.

It is also possible to interpret the obtained results in a reversed relation. For example, at  $I/I_n = 1.2$  relative temperature of the system without the heat sink was  $T/T_n \approx 1.3$ , but for the optimal porous cooling structure ( $k_v = 0.6$ ) it was  $T/T_n = 0.95$ . In this variant, the coil's operating conditions will be preserved. Furthermore, mean time between failures will lengthen since critical operating conditions will not be achieved.

According to formula (5.7) we calculated the cooling effectiveness which is a relative temperature decrease of the element for different supply currents. An optimal porous heat sink was able to reduce (at  $I = 0.5I_n$ ) mean temperature of the coil by 12.5% with relation to the system without any cooling device and 4% to the system with the uniform heat sink. This effectiveness increased with increasing current, hence at  $I = 2I_n$  the temperature was decreased by 25.4% and 6.68% respectively. The obtained characteristics (Fig. 5.6 and Fig. 5.7) indicate that the cooling effectiveness of porous heat sinks raises at higher current values. The optimal porous structure is even more effective than the uniform one. This may lead to mass reduction, where after applying the porous heat sink there is a possibility to use 80% less material ( $k_v = 0.2$ ) and preserve similar cooling performance (Fig. 5.4, Fig. 5.6) as a homogeneous plate.

# Conclusions

The paper presents an analysis and the results of the thermal operation conditions of an exemplary, conventionally cooled electronic device. The cooling effectiveness of an axial coil is discussed, before and after the periodic low-power heat sink with modified internal geometry was applied. Several different thermal conditions, at which a coil was operating, were investigated and analyzed. The electronic device, supplied by the low frequency AC current, was combined with planar cooling structures. In addition, some cases where the coil was carrying current different than nominal were considered. Then, we compared the cooling effectiveness of the homogeneous plate and porous, periodic heat sinks. Numerical calculations of the model were performed by finite element method (FEM), in order to solve the conjugate heat transfer field problem, simulated in a three-dimensional coordinate system.

The numerical results indicate very different thermal field distributions at the surface of the entire model for the cases, where planar cooling structures with different geometries were simulated. The application of these porous heat sinks allowed for lowering the temperature of the electronic device by 20%, compared with the case without heat sink. The discussed structures were also at least 6% more effective at cooling the coil than the homogeneous copper plate. Furthermore, the cooling effectiveness of the axial coil rose with higher values of the supplying current, which theoretically allows for overloading the device with current higher than nominal. In this situation, mean temperature may be reduced by 25% compared with the case without the heat sink. The porous heat sink gives an ability to achieve better or at least identical cooling effectiveness such as the homogeneous one, however, periodic porous structures have less weight, which introduces material savings and the use of the laminate's surface.

This work was supported by Ministry of Science and Higher Education in Poland under work No. WZ/WE-IA/2/2020.

**Authors:** A. Steckiewicz (e-mail: a.steckiewicz@pb.edu.pl), G. Druć (e-mail: gabriela.druc2d@gmail.com), J. M. Stankiewicz (e-mail: j.stankiewicz@doktoranci.pb.edu.pl), Białystok University of Technology, Faculty of Electrical Engineering, Wiejska 45D Str., 15-351 Białystok, Poland.

## References

- [1] Y. Liu, "Power electronic packaging: design, assembly process, reliability and modeling," New York, USA: Springer, 2012.
- [2] S. Horton, "PCB-cooling techniques and strategies for IC packages," *Electronic Products*, April 2011. [Online]. Accessed: [https://www.electronicproducts.com/Thermal\\_Management/Heat\\_Sinks\\_and\\_Thermal\\_Materials/PCB-cooling\\_techniques\\_and\\_strategies\\_for\\_IC\\_packages.aspx](https://www.electronicproducts.com/Thermal_Management/Heat_Sinks_and_Thermal_Materials/PCB-cooling_techniques_and_strategies_for_IC_packages.aspx).
- [3] P. Górecki, "Radiatory część 3," *Elektronika Praktyczna*, Vol. 5, No. 94, 1994.
- [4] D. Shamvedi, O.J. McCarthy, E. O'Donoghue, C. Danilenkoff, P. O'Leary and R. Raghavendra, "3D Metal printed heat sinks with longitudinally varying lattice structure sizes using direct metal laser sintering," *Virtual and Physical Prototyping*, Vol. 13, No. 4, 2018.

- [5] G. Langer, M. Leitgeb, J. Nicolics, M. Unger, H. Hoschopf and F. Wenzl, "Advanced Thermal Management Solutions on PCBs for High Power Applications," *Journal of Microelectronics and Electronic Packaging*, Vol. 11, No. 3, 2014.
- [6] A.S. Koohbanani, M. Ahmadi and M. Bahrami, "Improving Thermal Performance of Printed Circuit Boards by Thermal VIAs," [in:] *Proc. 43<sup>rd</sup> Annual Conference of North American Thermal Analysis Society*, Montreal, Canada, 2015.
- [7] N. Kafadarova and A. Andonova, "PCB thermal design improvement through thermal vias," [in:] *Proc. of the 8<sup>th</sup> WSEAS International Conference on Circuits, Systems, Electronics, Control & Signal Processing (CSECS '09)*, Tenerife, Spain, 2009.
- [8] A.C. Yunus and J.G. Afshin, "Heat and Mass Transfer: Fundamentals and Applications," 5<sup>th</sup> edition, New York, USA: McGraw-Hill, 2015.
- [9] A. Fan, R. Bonner, S. Sherratt and Y. Sungataek Ju, "An Innovative Passive Cooling Method for High Performance Light-emitting Diodes," [in:] *Proc. 28<sup>th</sup> IEEE SEMI-THERM Symposium*, March 2012, pp. 319–324.
- [10] W.W. Wits, "Integrated cooling concepts for printed circuit boards," Ph.D. dissertation, Faculty of Engineering Technology (CTW), University of Twente, Enschede, Netherlands, 2008.
- [11] P. Górecki, "Radiatory w sprzęcie elektronicznym," *Elektronika dla Wszystkich*, Vol. 12, No. 99, 1999.
- [12] M. Zareba, "Application of Duhamel's Theorem in the Analysis of the Thermal Field of a Rectangular Busbar," *Journal of Electrical Engineering and Technology*, Vol. 14, No. 1, 2019.
- [13] M. Zareba, "Comparison of heating curves of a rectangular busbar in different conditions of heat abstraction during the short-circuit heating," *Bulletin of the Polish Academy of Sciences. Technical Sciences*, Vol. 66, No. 1, 2018.
- [14] Choroszucho, "Analysis of the influence of the complex structure of clay hollow bricks on the values of electric field intensity by using the FDTD method," *Archives of Electrical Engineering*, Vol. 65, No. 4, 2016.
- [15] K. Siwek and S. Osowski, "Particle swarm optimization in synthesis of electric circuits," [in:] *Proc. 17<sup>th</sup> International Conference Computational Problems of Electrical Engineering (CPEE)*, Sandomierz, Poland, 2016.
- [16] M. Taya, "A constrained discrete layer model for heat conduction in laminated composites," *Computers & Structures*, Vol. 83, No. 21–22, pp. 1705–1718, 2005.